ELSEVIER

Journal of Environmental Management 77 (2005) 35–46

Journal of
Environmental
Management

www.elsevier.com/locate/jenvman

Modelling of geochemical reactions and experimental cation exchange in MX80 bentonite

G. Montes-H[a,*], B. Fritz[a], A. Clement[a], N. Michau[b]

[a]*UMR 7517 ULP-CNRS, CGS, 1 rue Blessig, F-67084 Strasbourg, France*
[b]*ANDRA, 1/7 rue Jean Monnet, 92298 Châtenay-Malabry cedex, France*

Received 15 May 2004; revised 11 January 2005; accepted 3 March 2005
Available online 8 June 2005

Abstract

Bentonites are widely used for waste repository systems because of their hydrodynamic, surface and chemical-retention properties. MX80 bentonite (bentonite of Wyoming) contains approximately 85% Na/Ca-montmorillonite and 15% accessory minerals. The dominant presence of Na/Ca-montmorillonite in this clay mineral could cause it to perform exceptionally well as an engineered barrier for a radioactive waste repository because this buffer material is expected to fill up by swelling the void between canisters containing waste and the surrounding ground. However, the Na/Ca-montmorillonite could be transformed to other clay minerals as a function of time under repository conditions. Previous modelling studies based on the hydrolysis reactions have shown that the Na/Ca-montmorillonite-to-Ca-montmorillonite conversion is the most significant chemical transformation. In fact, this chemical process appears to be a simple cation exchange into the engineered barrier.

The purpose of the present study was two-fold. Firstly, it was hoped to predict the newly formed products of bentonite-fluid reactions under repository conditions by applying a thermokinetic hydrochemical code (KIRMAT: Kinetic Reactions and Mass Transport). The system modelled herein was considered to consist of a 1-m thick zone of water-saturated engineered barrier. This non-equilibrated system was placed in contact with a geological fluid on one side, which was then allowed to diffuse into the barrier, while the other side was kept in contact with iron-charged water. Reducing initial conditions ($P_{O_2} \cong 0$; $Eh = -200$ mV) and a constant reaction temperature (100 °C) were considered.

Secondly, it was hoped to estimate the influence of interlayer cations (Ca and Na) on the swelling behaviour of the MX80 bentonite by using an isothermal system of water vapour adsorption and an environmental scanning electron microscope (ESEM) coupled with a digital image analysis (DIA) program. Here, the MX80 bentonite was previously treated with concentrated solutions (1 N) of calcium and sodium chlorides.

The results confirmed that the Na/Ca-montmorillonite-to-Ca-montmorillonite conversion was the main chemical transformation in the bentonite barrier under repository conditions. A simplified method (based on volume balance) has shown that the swelling capacity of the engineered barrier would be slightly affected after 1000 years of diffusion-reaction because the volume of neo-formed swelling clays is almost directly proportional to the volume of transformed initial-montmorillonite. Minimal neo-formation of saponites, vermiculites and chlorites was also observed. In addition, an isothermal system of water adsorption and ESEM-DIA methods showed that in the raw-bentonite-to-Ca-bentonite exchange there is a small decrease in the amount of adsorbed water and the swelling potential.

Keywords: Engineered barrier; MX80 bentonite; Swelling; Modelling; Geochemical transformations; Interlayer cation; Mass transport; ESEM; Digital image analysis

1. Introduction

In the general concept of radioactive waste disposal, it is proposed to store waste in deep geological layers of impervious clay. Vitrified waste is laid in canisters in the middle of a gallery dug in the clay formations. In order to protect the canisters from water intrusion, and to eventually trap released radioelements, waste-forms will be isolated

* Corresponding author. Tel.: +33 390 240 445; fax: +33 390 240402.
E-mail addresses: montes@illite.u-strasbg.fr (G. Montes-H), german_montes@hotmail.com (G. Montes-H).

0301-4797/$ - see front matter © 2005 Elsevier Ltd. All rights reserved.
doi:10.1016/j.jenvman.2005.03.003

from the surrounding geological media by two barriers: (a) the steel canister, and (b) an engineered backfill barrier system. This backfill barrier will be essentially composed of compacted clay blocks because of the hydrodynamic and surface properties of clay materials. In addition, the swelling characteristics of the buffer material are expected to fill up the void between the canisters containing the waste and the surrounding ground, and to build a better impermeable zone around high-level radioactive wastes. This role is called 'self-sealing' (Komine, 2004; Komine and Ogata, 2003).

Na/Ca-montmorillonite is the main mineral phase in MX80 bentonite (approximately 85%) (Sauzéat et al., 2001). Consequently, this clay material could perform exceptionally well as an engineered barrier for a radioactive waste repository because of its swelling properties (see Fig. 1). However, the Na/Ca-montmorillonite could be transformed to other clay minerals as a function of time under repository conditions. Preliminary modelling studies have shown that the Na/Ca-montmorillonite-to-Ca-montmorillonite conversion was the most significant chemical transformation (swelling clays). A minimal neo-formation of chlorites (non-swelling clays) was also identified in simulations as a potential chemical transformation, in particular near to the iron container (Kluska et al., 2002; Montes-H et al., 2004).

The current study served two purposes: (1) To estimate the neo-formed phases resulting from bentonite dissolution under repository conditions by applying a thermokinetic hydrochemical code (KIRMAT: Kinetic Reactions and Mass Transport) (Gérard et al., 1998). The system modelled was considered to consist of a 1-m thick zone of water-saturated engineered barrier. This non-equilibrated system was placed in contact with a geological fluid on one side, which was then allowed to diffuse into the barrier, while the other side was kept in contact with iron-charged water. This configuration represented the contact of an engineered barrier with a geological medium and with a container in a geological disposal facility for radioactive wastes (Fig. 2).

A grid spacing of 5 cm was used for all the calculations reported, i.e. the thick zone of the engineered barrier was divided into 20 grids. Reducing initial conditions ($P_{O_2} \cong 0$; $Eh = -200$ mV) and a constant reaction temperature (100 °C) were considered.

(2) Previous modelling studies based on the hydrolysis reactions have shown that the Na/Ca-montmorillonite-to-Ca-montmorillonite conversion is the most significant chemical transformation under repository conditions. In fact, this chemical process seems to be a simple cation exchange in the engineered barrier. Consequently, the present study focussed on estimating the influence of

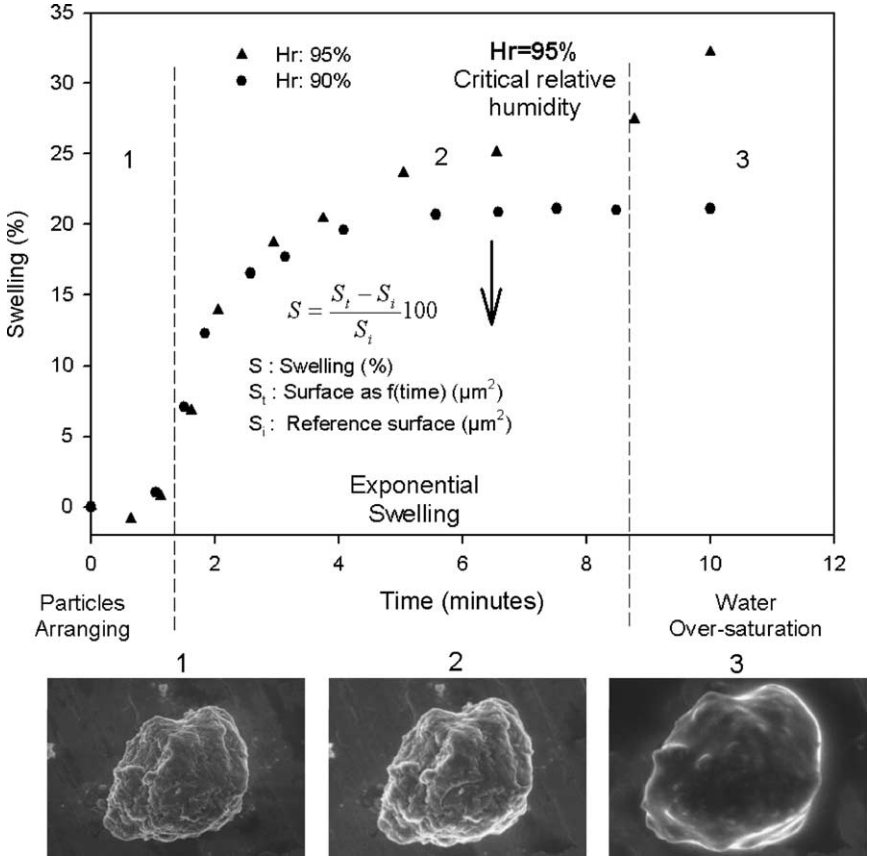

Fig. 1. Swelling kinetic behaviour of MX80 bentonite 'aggregate scale'. Determination by coupled ESEM-DIA (after Montes-H, 2003a).

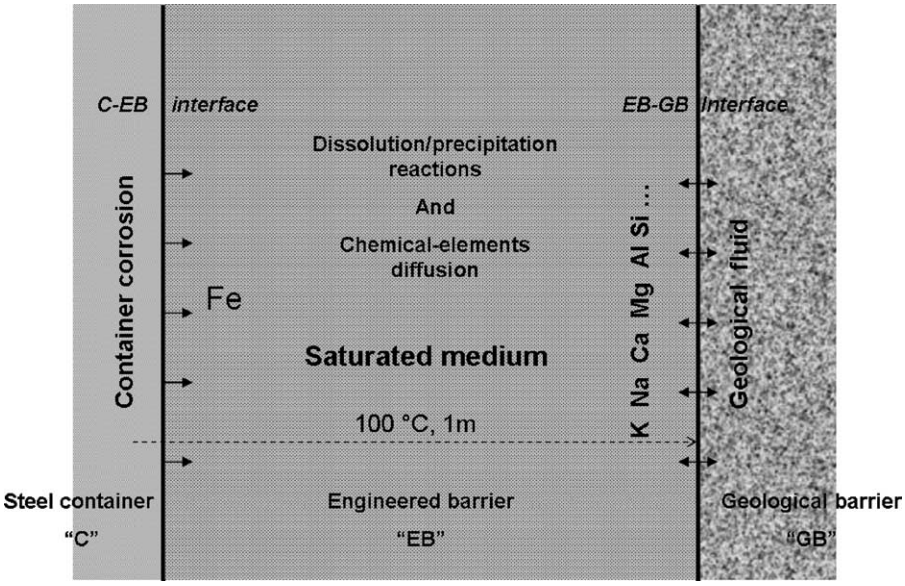

Fig. 2. Schematic representation of fluid-bentonite reaction and solute diffusion in an engineered barrier for radioactive waste confinement.

interlayer cations (Ca and Na) on the swelling behaviour of the MX80 bentonite by using an isothermal system of water vapour adsorption and an environmental scanning electron microscope (ESEM) coupled with a digital image analysis (DIA) program (Montes-H, 2003a; Montes-H and Geraud, 2004). The MX80 bentonite was previously treated with concentrated solutions (1N) of calcium and sodium chlorides (see Section 3).

2. Simulation

2.1. Model description

The Eulerian thermokinetic hydrochemical code KIRMAT (Gérard et al., 1998) was developed from the single-reaction path model KINDIS (Madé et al., 1994), by using its geochemical formulation and its numerical method to solve chemical equations.

The thermokinetic geochemical code KINDIS was developed from the purely thermodynamic code DISSOL (Fritz, 1975, 1981; Fritz and Tardy, 1976), which in turn originated from PATH1 (Helgeson et al., 1970). Theoretical kinetic rate laws for mineral dissolution and precipitation based on the Transition State Theory (TST) have been implemented in DISSOL. These geochemical codes have been intensively numerically tested and used in published studies on hydrothermal, diagenetic and weathering processes (e.g. Nöack et al., 1993; Bertrand et al., 1994).

In KINDIS, the irreversible kinetic driving force is explicitly calculated and the sequence of partial equilibrium states is calculated from second-order Taylor series expansion (Madé et al., 1994).

In KIRMAT, solute transport is added to kinetic dissolution and/or precipitation reactions. A chemically controlled time step (denoted Δt_c) allows preservation of accuracy of the calculations. Its value is inversely proportional to the largest of the first derivative variations among all the solute concentrations, and is controlled by setting the θ parameter (inversely proportional to Δt_c). The set of partial differential equations is integrated along one direction using the classical finite difference approximation method. An explicit scheme and a one-step algorithm are used to simultaneously solve the chemical (from KINDIS) and the conservative transport mass balance equations. A classical mixing cell scheme, the explicit-backward discretization, is computed for a numerical validation study.

The coupling of chemical reactions with mass transport is currently reported in the literature. Unfortunately it is still difficult to take into account all physico-chemical phenomena in a system (Steefel and Lasaga, 1990; Poinssot and Toulhoat, 1998; Collin et al., 2002; Gens et al., 2002; Keijzer et al., 1999; Malusis and Shackelford, 2002; Ulm et al., 2002; Le Gallo et al., 1998; Savage et al., 2002; Hökmark et al., 1997; Carnahan, 1992; Kälvenius and Ekberg, 2003).

2.2. General considerations

All simulations presented herein were performed using version 1.6 of the thermokinetic hydrochemical code KIRMAT (Gérard et al., 1998). The main interest was to simulate the geochemical transformations of the engineered barrier (hydrolysis reactions), taking into account the diffusion of chemical elements (mainly Fe, K, Ca, Na and Mg). The following aspects were considered to simplify the modelling system.

2.2.1. (i) Geochemical transformations in a fluid-saturated medium

A recent study showed that a bentonite barrier is fully water-saturated within approximately 3–4 years after deposition (Hökmark, 2004). It was supposed that the interface contact 'engineered barrier-geological medium' operates as a permeable membrane only to the water during the hydration phase of the engineered barrier. In this case, the chemical species contained in the geological fluid will only be adsorbed (or retarded) in the first few centimeters of the engineered barrier. This allows the assumption that initially the engineered barrier is saturated with a fluid of low concentration. In the present study, the engineered barrier is initially saturated with pure water.

2.2.2. Solute diffusion

In the water-saturated engineered barrier of bentonite, the interstitial fluid is almost static because of the very low permeability in the medium. In these conditions the convection transport can be negligible. Then, the significant transport phenomenon through the engineered barrier is uniquely the diffusion of chemical elements, mainly iron diffusion toward the geological medium, and K, Ca, Na, Si, etc. diffusion toward the metallic container.

2.2.3. Reducing conditions

Following the closing of the repository system, the hydrolysis reactions of the mineral constituents of the engineered barrier take place in reducing conditions ($P_{O_2} \cong 0$; $Eh = -200$ mV) because the oxygen is consumed rapidly.

2.2.4. Container corrosion

In the KIRMAT code, it is difficult to take the container corrosion directly into account. Therefore, a significant concentration of total iron [0.001 mol/kg H_2O] was considered at the boundaries of the container. This means that one side of the engineered barrier is perturbed by a constant source of iron during the simulation. Unfortunately, this assumption could produce an acidification phenomenon in the system.

2.2.5. Initial state of the engineered barrier

The engineered barrier was considered initially to be in disequilibrium with the interacting solution (pure water). Therefore, this system was initially very reactive.

2.3. Input data

2.3.1. Primary minerals

MX80 bentonite has been widely studied by Sauzeat et al. (2001); Guillaume (2002); Montes-H (2002, 2003a,b, 2004); Tournassat et al. (2003); Neaman et al. (2003), and others. The mineral composition of this material is presented in Table 1. In the present study, the minerals contained in the MX80 bentonite were considered as primary minerals or as reactants for possible mineral dissolution or chemical transformation. In the KIRMAT simulations, the dissolution of primary minerals was calculated by using the kinetic reactions. In contrast, their precipitation was calculated by applying the themodynamic equilibrium conditions.

2.3.2. Secondary minerals

The secondary minerals or neo-formed mineral phases were chosen following the conclusions of the laboratory experiments conducted at 80 and 300 °C, in the presence of metallic iron (Guillaume, 2002). Table 2 presents the secondary minerals considered in the KIRMAT simulations. The secondary mineral precipitation (or neo-formation) was calculated by applying the themodynamic equilibrium conditions (i.e. equilibrium condition for precipitation).

2.3.3. Initial composition of fluid

The engineered barrier was considered as a saturated medium, initially saturated with pure water. In contrast, the geological fluid was a representative geological fluid of the French Callovo–Oxfordian Formation (see Table 3).

2.3.4. Temperature of reaction

In the KIRMAT code, it is not possible to take into account the temperature gradient as a function of time produced by the disintegration reactions of radioactive wastes. However, it is

Table 1
Mineral composition of MX80 bentonite (Sauzeat et al., 2001); and thermodynamic equilibrium constants used in KIRMAT simulations

Mineral	Volume fraction (Dry bentonite)	Volume fraction water-saturated Bentonite	Chemical formula	Log(K_m) (100 °C)
Pyrite	0.00313	0.002023	FeS_2	−67.89[a]
Calcite	0.00966	0.006245	$CaCO_3$	−9.39[a]
Quartz	0.07032	0.045465	SiO_2	−3.095[a]
Microcline	0.01066	0.006892	$KAlSi_3O_8$	−18.104[a]
Albite	0.03490	0.022564	$NaAlSi_3O_8$	−16.037[a]
Biotite	0.02783	0.017993	$K(Fe_3)[Si_3AlO_{10}](OH)_2$	5.910[a]
Montmorillonite	0.84350	0.898814	$[Si_{3.98}Al_{0.02}O_{10}](OH)_2$ $(Al_{1.55}Mg_{0.28}Fe^{III}_{0.09}Fe^{II}_{0.08})$ $(Na_{0.18}Ca_{0.10})$	−28.455[b]
Total	1	1		

[a] Data base of KIRMAT code.
[b] The sum of polyhedral contributions (Chermak, 1989, 1990).

Table 2
Secondary minerals and the thermodynamic equilibrium constants used in KIRMAT simulations

Mineral	Chemical formula	Log(K_m) (100 °C)
Vermiculite	$[(Si_{7.34}Al_{0.66}O_{20})(OH)_4]$	−5.14[a]
MgFe2	$(Al_{0.66}Fe^{II}_{2.3}Mg_{3.04})$	
Saponite Fe(II)	$[(Si_{7.34}Al_{0.66}O_{20})(OH)_4]$ $(Fe^{II}_6)Na_{0.66}$	−2.05[a]
Saponite	$[(Si_7AlO_{20})(OH)_4]$	−2.11[a]
MgFe(II)	$(Al_{0.5}Fe^{II}_{2.5}Mg_3)Ca_{0.1}Na_{0.3}$	
Smectite_Na	$[(Si_{7.92}Al_{0.08}O_{20})(OH)_4]$ $(Al_{3.04}\ Fe^{III}_{0.36}Mg_{0.54})Na_{0.8}$	−28.84[a]
Smectite_Ca	$[(Si_{7.92}Al_{0.08}O_{20})(OH)_4]$ $(Al_{3.04}\ Fe^{III}_{0.36}Mg_{0.54})Ca_{0.4}$	−29.23[a]
Phillipsite Na	$[Si_{10}Al_6O_{32}]Na_5Ca_{0.5}12H_2O$	−72.05[a]
Laumonite	$[SiAl_2O_8]Ca,4H_2O$	−26.38[b]
Chabazite Na	$[Si_8Al_4O_{24}]Na_{3.5}Ca_{0.2}13H_2O$	−51.26[a]
Chlorite FeAl	$[Si_2Al_2O_{10}(OH)_2](Fe^{II}Al_2)(Fe^{II}{}_3)(OH)_6$	−55.57[a]
Chlorite MgAl	$[Si_2Al_2O_{10}(OH)_2](MgAl_2)(Mg_3)(OH)_6$	−31.23[a]
Illite	$[(Si_{3.5}Al_{0.5}O_{10})(OH)_2](Al_{1.8}Mg_{0.25})K_{0.6}$	−35.23[b]
Goethite	$FeO(OH)$	8.82[b]
Siderite	$FeCO_3$	−11.95[b]
Magnetite	Fe_3O_4	−3.39[b]
Anhydrite	$CaSO_4$	−5.36[b]
Gypsum	$CaSO_4 \cdot 2H_2O$	−5.010[b]
Thenardite	Na_2SO_4	−0.640[b]
Jarosite	$KFe^{III}{}_3(SO_4)_2(OH)_6$	20.84[b]

[a] The sum of polyhedral contributions (Chermak, 1989, 1990).
[b] Data base of KINDISP model.

possible to take into account any temperature between 0 and 300 °C. The confinement barrier is subjected to temperature variations (>70 °C and sometimes >100 °C) (Collin et al., 2002). In the present study, a constant temperature of 100 °C as a function of time was assumed.

2.3.5. Initial pH and P_{O_2}

P_{O_2} was initially fixed at 3.16×10^{-4} bar. Knowing that the alkaline reserve is close to zero for pure water, the initial pH was calculated at 5.89 considering a temperature of 100 °C.

Table 3
Chemical composition, pH and Eh of a representative geological fluid from Callovo-Oxfordian formation (Jacquot, 2002)

Chemical parameters	Value	Observation
Eh [mV]	−185	SO_4/pyrite equilibrium
PH	7.30	Electroneutrality condition
Na [mol/kg H_2O]	4.17×10^{-2}	Na–Ca exchange
K [mol/kg H_2O]	5.40×10^{-3}	K–Ca exchange
Ca [mol/kg H_2O]	9.74×10^{-3}	Equilibrium with calcite
Mg [mol/kg H_2O]	7.68×10^{-3}	Na–Mg exchange
SiO_{2aq} [mol/kg H_2O]	9.44×10^{-5}	Equilibrium with quartz
Cl [mol/kg H_2O]	7.19×10^{-2}	Calculated by lixivation
SO_4 [mol/kg H_2O]	4.40×10^{-3}	$pCO_2=3.09\times10^{-3}$ condition
Al [mol/kg H_2O]	9.26×10^{-9}	Equilibrium with illite
Fe [mol/kg H_2O]	6.44×10^{-5}	Equilibrium with daphnite
C_T(Inorganic) [mol/kg H_2O]	1.44×10^{-3}	Equilibrium with dolomite
pCO_2 [atm]	3.09×10^{-3}	–

2.3.6. Water-rock ratio

The total physical porosity of MX80 bentonite was estimated at 30% (Sauzeat et al., 2001). Assuming that the engineered barrier was initially saturated with pure water and knowing that the KIRMAT code was based on 1 kg of water (i.e. approximately 1000 cm^3 'V_{water}'), it was very easy to estimate the volume of rock involved in the interaction (approximately 2333 cm^3). This value, the mineral volume fraction of the dry bentonite, and the swelling potential of Na/Ca-montmorillonite, allow the calculation of the initial volume of each primary mineral in the system.

2.3.7. Thermodynamic equilibrium constants

The KIRMAT code is based on hydrolysis reactions where the major aqueous species are mainly H_4SiO_4, $Al(OH)_4^-$, CO_3^{2-}, SO_4^{2-}, Na^+, K^+, Ca^{2+}, Mg^{2+}, Fe^{2+}, Fe^{3+}, H^+ and H_2O. The thermodynamic equilibrium constants of the hydrolysis reactions used in KIRMAT simulations at 100 °C are presented in Tables 1 and 2.

2.3.8. Kinetic data

The simplified equation used to simulate the dissolution rate of a mineral *m* in the KIRMAT code may be written as:

$$v^s_{dm} = k^{pH}_{dm} S^{eff}_m a^n_{H+}\left(1-\frac{Q_m}{K_m}\right) \quad (1)$$

where k^{pH}_{dm} is the constant of the apparent dissolution rate intrinsic to mineral m at a given pH [mol/m^2/year]; S^{eff}_m is the effective or reactive surface area (as a function of the number of actives sites) at the mineral/aqueous solution interface [m^2/kg H_2O]; $a^n_{H^+}$ is the activity of the H^+ ions in the aqueous solution, where *n* is a real exponent with a generally positive value in acid solutions, zero in neutral solutions and negative in basic solutions; $(1-Q_m/K_m)$ is the saturation index of mineral m in an aqueous solution, where Q_m is the ionic activity product and K_m is the thermodynamic equilibrium constant known for the given temperature and pressure conditions.

The intrinsic constant of mineral dissolution (k^{pH}_{dm}) is a function of the temperature, and can be described by the Arrhenius law:

$$k^{pH}_{dm} = A_m \exp\left(\frac{-E_{am}}{RT}\right) \quad (2)$$

with A_m being the frequency factor and E_{am} the activation energy of the mineral dissolution reaction [J/mol].

The k^{pH}_{dm} data used in the current study were taken from studies by Jacquot (2000); Kluska and Fritz (2001). These values are summarized in Table 4.

Conversely, the effective or reactive surface area (S^{eff}_m) could be defined as a percentage of the total mineral surface

Table 4
The kinetic data used in the KIRMAT simulations

Mineral	S_m^{eff} (*)	k_{dm}^{pH} [mol/m^2.year]			PH limit	
	[m^2/kg H_2O]	k^H (*)	k^{H2O} (*)	k^{OH} (*)	*A-to-N*	*N-to-B*
Pyrite	2.19	1.88×10^{-18}	1.88×10^{-18}	1.88×10^{-18}	–	–
Calcite	6.76	7.93×10^{6}	8.69×10^{2}	8.69×10^{2}	4.4	8.3
Quartz	49.22	4.5×10^{-3}	1.7×10^{-3}	3.18×10^{-6}	2	5.5
Microcline	7.46	1.40	7.89×10^{-3}	5.97×10^{-6}	4.5	7.8
Albite	24.42	1.40	7.89×10^{-3}	5.97×10^{-6}	4.5	7.8
Biotite	19.48	1.34×10^{-3}	1.89×10^{-5}	5.45×10^{-7}	5	7
Montmorillonite	590.4	1.34×10^{-3}	1.89×10^{-5}	5.45×10^{-7}	5	7

k^H, constant of the dissolution rate in an acid medium; k^{H2O}: constant of the dissolution rate in a neutral medium, independent of the pH. k^{OH}, constant of the dissolution rate in a basic medium; S_m^{eff}, reactive surface area; A, acid; N, neutral; B, basic; * kinetic data (after compilation made by Jaquot, 2000; Kluska and Fritz, 2001).

area, generally between 50 and 90% (White and Peterson, 1990). Recently, atomic force microscopic experiments showed that only 8–14% of the total mineral surface area participates as a reactive surface area (S_m^{eff}) in the dissolution of several silicates (Nagy et al., 1999; Tournassat et al., 2003). It is still difficult to estimate with precision the reactive surface area of silicates and phyllosilicates. Granular studies show that a bulk sample of MX80 bentonite is composed of 86.1% of particles <2 μm in size, 8.8% in the 2–50-μm range and 5.1% >50 μm (Neaman et al., 2003). In the present study, it was assumed that the MX80 bentonite was composed of particles of 2 μm in size. This consideration allowed the calculation of the total mineral surface area (S_m^T) for each primary mineral. Finally, it was also assumed that only 10% of the total mineral surface area participated as a reactive surface area ($S_m^{eff} = 0.1S_m^T$).

The kinetic data (k_{dm}^{pH}, S_m^{eff}) used in the KIRMAT simulations are presented in Table 4.

2.3.9. Diffusion coefficient

The transport of solutes into the clay barrier was considered to be a pure diffusion process in a saturated medium. The initial effective coefficient of diffusion tested in the simulations was 10^{-11} m^2/s. This value was selected based on published data for compacted MX80 (Lehikoinen et al., 1996). The KIRMAT code uses the same value for all chemical species and considers a constant molecular diffusion.

3. Experimental methods

3.1. Cation saturation

In order to determine the effect of exchanged cations, the bulk samples of MX80 bentonite were treated separately with two concentrated solutions (1-N concentration) of sodium and calcium chlorides. These salts have the same ionic force ($I=2$).

Twenty grams of MX80 bentonite was dispersed into 1 L of salt solution (1 N) at 60 °C. This suspension was vigorously stirred using magnetic agitation for 1 h at 60 °C. Then, the cation-saturated clay was separated by centrifugation (15 min at 13,000 rpm) and decanting of the supernatant solutions. This process was repeated three times. The cation-saturated bentonite was then washed three to four times with distilled water until the $AgNO_3$ test for chloride was negative (method used by Lee and Kim (2002); Rytwo (1996)). The cation-saturated bentonite was subsequently dried for 48 h at 60 °C and finally ground for 2 min.

3.2. Isothermal water sorption

Adsorption/desorption isotherms of water vapour at 23 °C were obtained using plastic desiccators (2 L) containing 1 g of sample (cation-saturated bentonite) previously dried for 24 h at 110 °C. Water activity was controlled with over-saturated salt solutions. These solutions were used to keep constant water activity of air in the plastic desiccators and surrounding sample contained in a glass jar.

The desiccators were kept at room temperature (23 °C). Weighing was done every 3 days using a digital balance (accuracy = 0.0001 g) until apparent equilibrium was reached (complete description by Montes-H (2003b))).

3.3. ESEM methodology

An XL30 ESEM LaB6 (FEI and Philips), fitted with a gaseous secondary electron detector (GSED) to produce a surface image, was used for all ESEM investigations. This microscope is also equipped with a ‘cooling stage’ to control the sample temperature.

Each sample was initially subjected to hydration and then a dehydration cycle, progressively increasing and decreasing the water activity. This process, coupled with the DIA, was used to estimate the swelling-shrinkage isotherm for each cation-saturated bentonite. A complete description of these methods was provided by Montes-H (2003a)) and Montes-H (2003b)).

4. Results and discussion

4.1. Chemical transformations in MX80 bentonite

Previous modelling studies carried out by the present institute have shown that the chemical transformations occurring in a bentonite barrier for radioactive waste confinement depend directly on the reaction temperature, the rate of iron corrosion, the composition of the interaction fluid, the nature and/or amount of accessory minerals, the diffusion coefficients of solutes and the reactive surface area of minerals (Kluska et al., 2002; Montes-H et al., 2004). In fact, the Na/Ca-montmorillonite-to-Ca-montmorillonite conversion was identified as the main chemical transformation in the bentonite barrier. This process represents a simple cation exchange phenomenon (see Fig. 3(a) and (b)). In Fig. 3(b), the chemical transformations of lesser impact can be observed in the engineered barrier. For example, there is a minimal neo-formation of chlorites, saponites and vermiculites.

4.2. Simplified method to evaluate the decay of swelling capacity

Due to its swelling properties, the buffer material is expected to fill up the spaces between the canisters containing the waste and the surrounding ground, and to

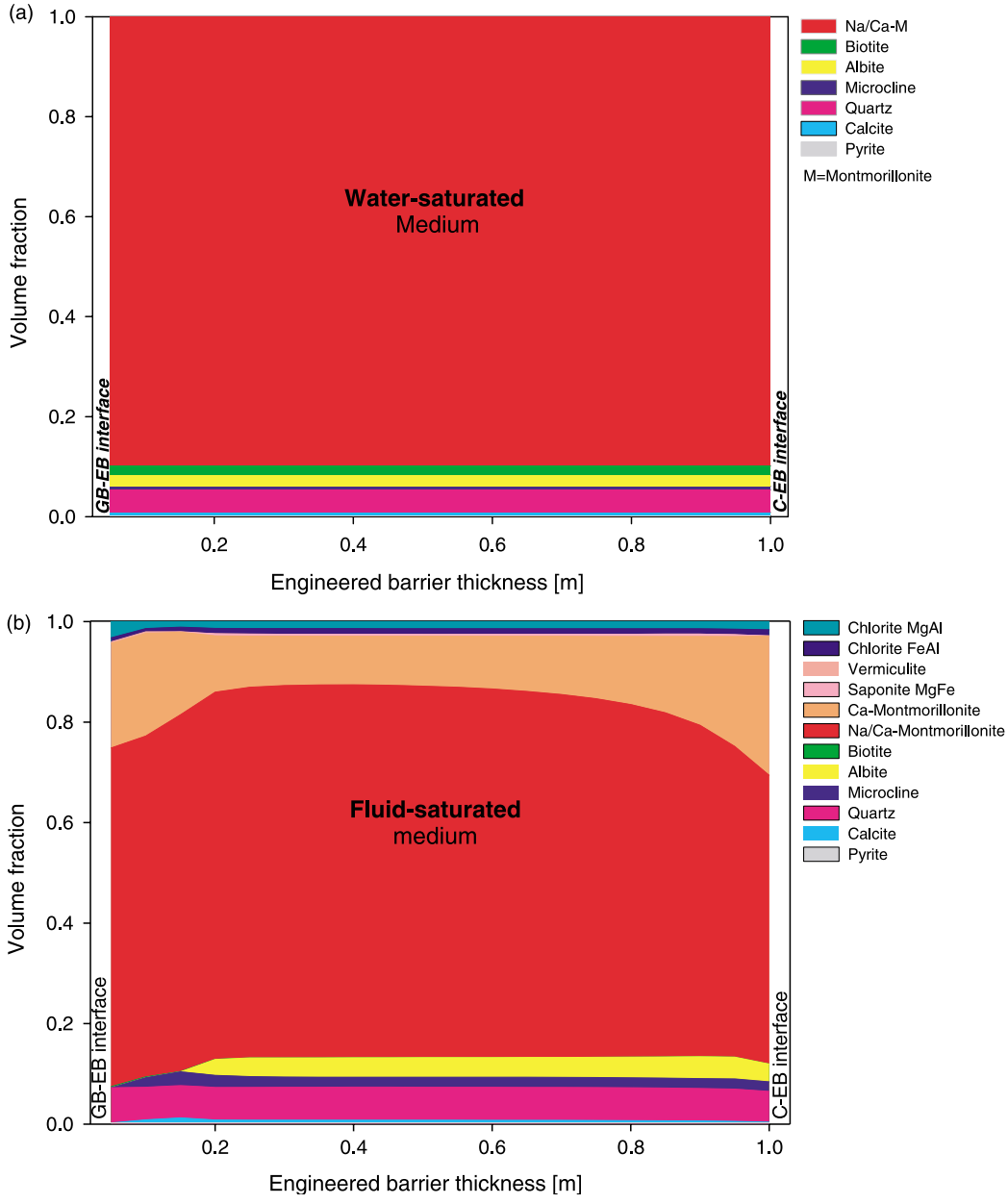

Fig. 3. (a) Mineral composition of water-saturated engineered barrier (initial state). (b) Mineral composition of fluid-saturated engineered barrier after 1000 years of diffusion-reaction (final state).

Table 5
Several physical properties of swelling clays

Swelling Clay	$\rho^{dry}_{sw\_clay}$ [gr/cm^3]	W [g/g$_{dryclay}$]	w [cm^3/cm^3]	S_w [cm^3/cm^3]	$\rho^{wet}_{sw\_clay}$ [gr/cm^3]	Molar mass [g/mol]	Molar volume [cm^3/mol]
Na/Ca–S	2.65	0.3	0.3	0.14	2.19	372.61	170
Na–S	2.65	0.37	0.3	0.3	2.10	373.14	178
Ca–S	2.65	0.25	0.3	0.1	2.18	371.96	171
Saponites	2.65	0.25	0.3	0.1	2.18	440.45*	202

$\rho^{dry}_{sw\_clay}$, Particle density of a dried swelling clay; W, Maximal amount of adsorbed water; w, Total physical porosity; S_w, The maximum swelling potential; $\rho^{wet}_{sw\_clay}$, Particle density of a hydrated swelling clay; S, Smectite; *Mean value between five different saponites.

build a more effective impermeable zone around high-level radioactive wastes. This role is known as 'self-sealing' and takes place in water-saturated conditions in a bentonite barrier. In this case, the specific (grain) densities of the non-swelling minerals remain constant. In contrast, the specific (grain) densities of the swelling minerals decrease because of their expansive property. Therefore, the specific (grain) density of a water-saturated swelling-clay can be calculated by the following expression:

$$\rho^{wet}_{sw\_clay} = \rho^{dry}_{sw\_clay}\left(\frac{1+W}{1+\frac{w}{1-w}+S_w}\right) \quad (3)$$

where $\rho^{dry}_{sw\_clay}$: specific (grain) density of a dried swelling clay. This value was estimated using the helium adsorption method (picnometry) for a bulk sample of MX80 bentonite (Sauzeat et al., 2001). In the current study, this value was considered as characteristic for any swelling clay. W is the maximal amount of adsorbed water. These values were estimated using the sorption kinetics of water vapour (HR = 95%) (Montes-H and Geraud, 2004). In the present study, it was assumed that the Ca-smectite and the saponites had the same capacity to adsorb the water vapour, w is the total physical porosity. This value was estimated using Hg-porosimetry for a bulk sample of MX80 bentonite (Sauzeat et al., 2001). In the present study, this value was considered as characteristic for any swelling clay. S_w is the maximum swelling potential. These values were estimated using a new technique coupling ESEM with a DIA program (Visilog) (Montes-H, 2003a). In the present study, it was assumed that the Ca-smectite and the saponites had the same swelling capacity.

The values used in the current study are summarized in Table 5. Based on its swelling properties, the clay was supposed to completely fill the total physical porosity of a bulk sample of bentonite buffer (see Fig. 4). In this case, the interstitial fluid was almost static because of the very low permeability in the medium. Consequently, only molecular diffusion was possible in the engineered barrier.

Conversely, it was considered that accessory minerals contained in the bulk bentonite do not affect the maximum swelling 'S_w' or the maximal amount of adsorbed water 'W'.

The specific (grain) density calculation for water-saturated swelling clays allows the estimation of their molar volume. This parameter is therefore used in the KIRMAT code to calculate the mineral volume in the system. This simple correction thus allowed the estimation of the decay of swelling capacity by a volume balance, considering that the decay of swelling capacity is directly

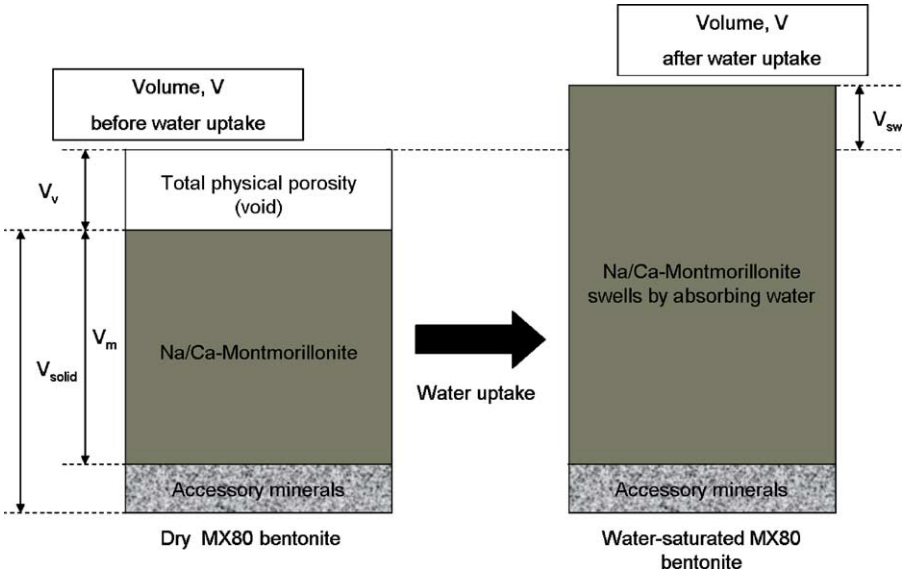

Fig. 4. Definition of MX80 bentonite barrier at water-saturated conditions (after Komine and Ogata, 2003).

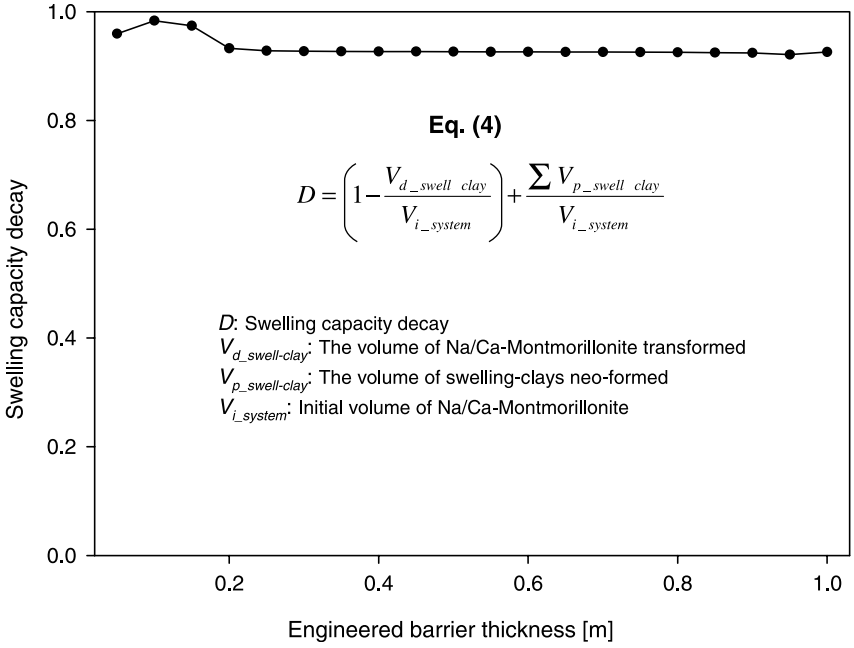

Fig. 5. Swelling capacity decay of the engineered barrier after 1000 years of diffusion-reaction.

proportional to the volume of transformed montmorillonite (cation exchange + geochemical transformations), taking into account that it may be partially compensated by the volume of neo-formed swelling clays. The calculation is then based on the following equation:

$$D = \left(1 - \frac{V_{\mathrm{d\_swell-clay}}}{V_{\mathrm{i\_system}}}\right) + \frac{\sum V_{\mathrm{p\_swell-clay}}}{V_{\mathrm{i\_system}}} \quad (4)$$

where $V_{\mathrm{d\_swell\text{-}clay}}$ is the volume of swelling-clay dissolution, $V_{\mathrm{p\_swell\text{-}clay}}$ is the volume of swelling-clay precipitation, and $V_{\mathrm{i\_sytem}}$ is the initial volume of swelling-clay in the system.

This simplified method (based on volume balance) shows that the swelling capacity of the bentonite barrier would be slightly affected after 1000 years of diffusion-reaction (D close to 1) because the volume of neo-formed swelling-clays is

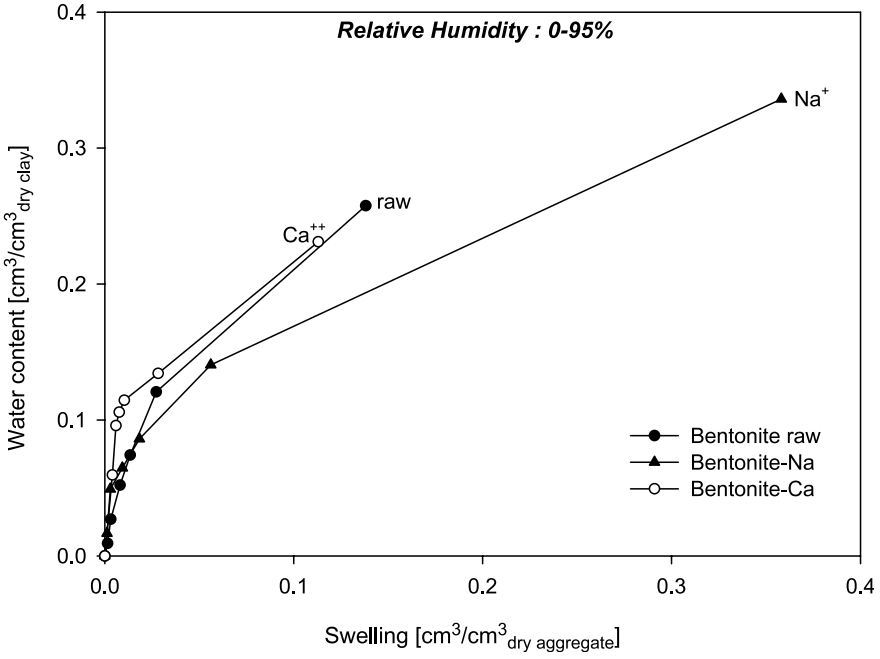

Fig. 6. Amount of adsorbed water and swelling potential correlation for raw and cation-saturated bentonite. The swelling potential was considered as equidimensional to aggregate scale.

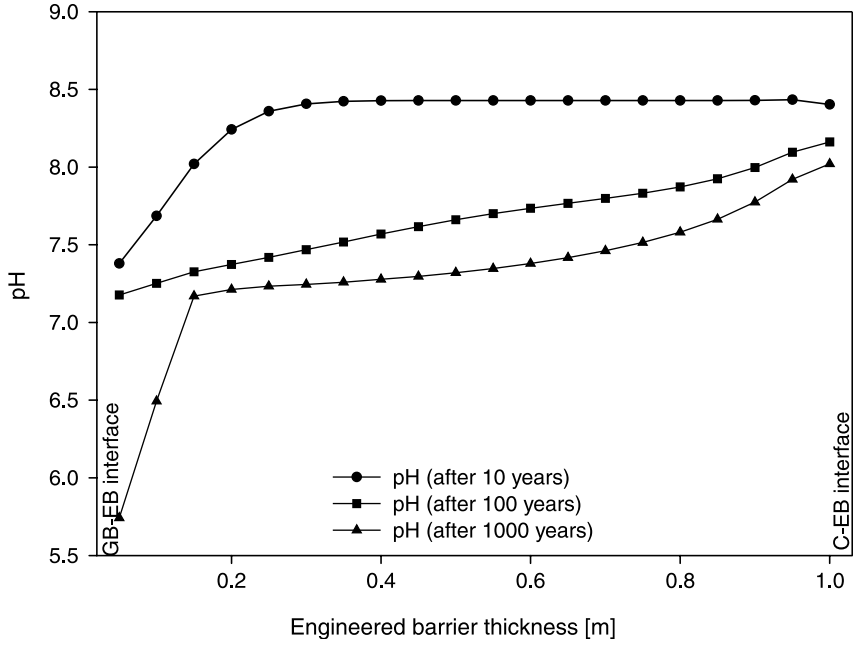

Fig. 7. pH evolution of the fluid interaction in the engineered barrier after 10, 100, and 1000 years of diffusion-reaction.

almost directly proportional to the volume of transformed Na/Ca-montmorillonite (see Fig. 5).

4.3. Correlation between amount of adsorbed water and swelling potential

Fig. 3 shows that the Na/Ca-montmorillonite-to-Ca-montmorillonite conversion is the main chemical transformation. This chemical process, identified by a hydrolysis reaction under repository conditions, seems to be a simple cation exchange phenomenon. Consequently, two experimental methods (isothermal adsorption of water and ESEM-DIA) were used in the present study, in order to estimate the influence of the interlayer cation on the montmorillonite contained in the MX80 bentonite. A quantitative correlation between the amount of adsorbed water and the swelling potential of raw and cation-saturated bentonite shows that these physical properties are governed by the nature of the interlayer cation. For example, the Na-saturated bentonite has an excellent capacity to adsorb water and to swell, while the Ca-saturated bentonite adsorbs water and swells less significantly. However, in the current study, the interesting comparison is between raw bentonite and Ca-saturated bentonite, where the effects are unremarkable. In fact, globally there is a small decrease in the amount of adsorbed water and the swelling potential (see Fig. 6).

4.4. pH evolution

Fig. 7 shows the pH evolution in the engineered barrier for the different times. Here, the pH is not homogeneous in the engineered barrier. In general, an acid pH was observed near the geological medium boundaries. This decrease in pH is due to a significant $[H^+]$ accumulation in the system, produced by the hydrolysis reactions of chlorites and saponites. Following this, the pH increases slightly to a value of 8.

5. Conclusion

The chemical transformations occurring in a bentonite barrier for radioactive waste confinement depend directly on the reaction temperature, the rate of iron corrosion, the composition of the interaction fluid, the nature and/or amount of accessory minerals, the diffusion coefficients of solutes, the reactive surface area of minerals and the texture of porous media. At the present time, it is difficult to efficiently consider all parameters in the same model, because of the complexity of their estimation. Consequently, the KIRMAT simulations were carried out under the drastic conditions found in a radioactive waste repository:

1. There was an infinite source and constant concentration of major cations in the boundaries of the geological medium. A constant concentration of total iron was also considered in the boundaries of the container.
2. The temperature of reaction, reactive surface area of minerals, diffusion coefficients of solutes and porosity were considered constants as a function of time and space.

The results show that the Na/Ca-montmorillonite-to-Ca-montmorillonite conversion was the main chemical transformation in the bentonite barrier. Other chemical

transformations of lesser impact were also identified in this barrier. For example, there was a minimal neo-formation of chlorites and saponites.

A simplified method shows that the swelling capacity of the engineered barrier would not be drastically affected after 1000 years of diffusion-reaction because the volume of neo-formed swelling-clays is almost directly proportional to the volume of transformed Na/Ca-montmorillonite. In addition, the isothermal system of water adsorption and ESEM-DIA methods have shown that in the raw-bentonite-to-Ca-bentonite exchange there is a small decrease in the amount of adsorbed water and the swelling potential.

The present study suggests that the bentonite barrier could preserve similar physical–chemical and mechanical properties after 1000 years of diffusion-reaction.

Acknowledgements

The authors are grateful to French national radioactive waste management agency (ANDRA), in the framework of its program on the geochemical behaviour of bentonite engineered barrier and National Council of Science and Technology (CONACYT, Mexico), for providing a financial support for this work.

References

Bertrand, C., Fritz, B., Sureau, J.-F., 1994. Hydrothermal experiments and themo-kinetic modelling of water–sandstone interactions. Chemical Geology 116, 189–202.

Carnahan, C.L., 1992. Numerical simulation of heterogeneous chemical reactions coupled to fluid flow in varying thermal field. Scientific Basis for Nuclear Waste Management XV Material Research Society Symposium Proceedings, vol. 257 pp. 683–690.

Chermak, J.A., Rimstidt, 1989. Estimating the thermodynamic properties (ΔG_f^0 and ΔH_f^0) of silicate minerals at 298 K from the sum of polyhedral contributions. American Mineralogist 74, 1023–1031.

Chermak, J.A., Rimstidt, 1990. Estimating the free energy of formation of silicate minerals at high temperatures from the sum of polyhedral contributions. American Mineralogist 75, 1376–1380.

Collin, F., Li, X.L., Radu, J.P., Chalier, R., 2002. Thermo-Hydro-mechanical coupling in clay barriers. Engineering Geology 64, 179–193.

Fritz, B., 1975. Etude themodynamique et simulation des reactions entre minéraux et solutions, Mémbrane Science Géology, vol. 41 1975 pp. 153.

Fritz, B., 1981. Etude thermodynamique et modélisation des réactions hydrothermales et diagénétiques. Mémbrane Science Géology 65, 197.

Fritz, B., Tardy, Y., 1976. Séquence de minéraux secondaires dans l'altération des granites et roches basiques: modèles thermodynamiques. Bulletin Society Géology, France 18, 7–12.

Gens, A., Guimaraes, L., Guimaraes, N., Garcia-Molina, A., Alonso, E.E., 2002. Factors controlling rock-clay buffer interaction in a radioactive waste repository. Engineering Geology 64, 297–308.

Gérard, F., Clement, A., Fritz, B., 1998. Numerical validation of a Eulerian hydrochemical code using a 1D multisolute mass transport system involving heterogeneous kinetically controlled reactions. Journal of Contaminant Hydrology 30, 201–216.

Guillaume D., 2002. Etude expérimentale du système fer-smectite en présence de solution à 80 °C et 300 °C. PhD Thesis, Henri Poincaré University, Nancy I, France, p. 210.

Helgeson, H.C., Brown, T.H., Nigrini, A., Jones, T.A., 1970. Calculations of mass transfer in geochemical processes involving aqueous solutions. Geochimical Cosmochim. Acta 34, 569–592.

Hökmark, H., 2004. Hydration of the bentonite buffer in a KBS-3 repository. Applied Clay Science 26, 219–233.

Hökmark, H., Karnland, O., Pusch, R., 1997. A technique for modeling transport/conversion processes applied to smectite-to-illite conversion in HLW buffers. Engineering Geology 47, 367–378.

Jacquot E., 2000. Modélisation thermodynamique et cinétique des réactions géochimiques entre fluides de bassin et socle cristallin. PhD Thesis, Louis Pasteur University, Strasbourg I, France, p. 202.

Jacquot E., 2002. Composition des eaux interstitielles des argilites du Callovo-Oxfordien non perturbées. Rapport ANDRA No. D NT ASTR 02-041, p. 13.

Kälvenius, G., Ekberg, C., 2003. TACK—a program coupling chemical kinetics with a two-dimensional transport model in geochemical systems. Computers Geosciences 29, 511–521.

Keijzer, Th.J.S., Kleingeld, P.J., Loch, J.P.G., 1999. Chemical osmosis in compacted clayed material and the prediction of water transport. Engineering Geology 53, 151–159.

Kluska J.M., Fritz B., 2001. Modélisation Thermodynamique et Cinétique des Réactions Géochimiques dans une Barrière Ouvragée en Bentonite. Simulations dans des conditions réductrices, de 60 à 180 °C en l'absence et en présence d'une source de fer sur une durée de 20 ans. Rapport ANDRA No. CRP 0CGS 01-004, p. 34.

Kluska J.M., Fritz B., Clement A., 2002. Predictions of the mineralogical transformations in a bentonite barrier surrounding an iron radioactive container. International meeting 'Clay in natural and engineered barriers for radioactive waste confinement' ANDRA, 8–12 December 2002, Reims, France.

Komine, H., 2004. Simplified evaluation for swelling characteristics of bentonites. Engineering Geology 71, 265–279.

Komine, H., Ogata, N., 2003. New equations for swelling characteristics of bentonite-based buffer materials. Canadian Geotechnical Journal 40, 460–475.

Lee, S.Y., Kim, S.J., 2002. Delamination behaviour of silicate layer by adsorption of cationic surfactants. Journal of Colloid and Interface Science 248, 231–238.

Le Gallo, Y., Bildtein, O., Brosse, E., 1998. Coupled reaction-flow modelling of diagenic changes in reservoir permeability, porosity and mineral compositions. Journal of Hydrology 209, 366–388.

Lehikoinen, J., Carlsson, J., Muurinen, A., Olin, M., Salonen, P., 1996. Evaluation of factors affecting diffusion in compacted bentonite. Material Research Society Symposium Proceedings 412, 675–682.

Madé, B., Clément, A., Fritz, B., 1994. Modelling mineral/solution interactions: the thermodynamic and kinetic code KINDISP. Computers and Geosciences 20 (9), 1347–1136.

Malusis, M.A., Shackelford, C.D., 2002. Theory for reactive solute transport through clay membrane barriers. Journal of Contaminant Hydrology 59, 291–316.

Montes-H G., 2002. Etude expérimentale de la sorption d'eau et du gonflement des argiles par microscopie électronique à balayage environnementale (ESEM) et analyse digitale d'images. PhD Thesis, Louis Pasteur University, Strasbourg I, France.

Montes-H, G., Geraud, Y., 2004. Sorption kinetic of water vapour of MX80 bentonite submitted to different physical-chemical and mechanical conditions. Colloids and Surfaces A: Physicochemical Engineering Aspects 235, 17–23.

Montes-H, G., Duplay, J., Martinez, L., Mendoza, C., 2003a. Swelling-shrinkage kinetics of MX80 bentonite. Applied Clay Science 22, 279–293.

Montes-H, G., Duplay, J., Martinez, L., Geraud, Y., Rousset-Tournier, B., 2003b. Influence of interlayer cations on the water sorption and swelling-shrinkage of MX80 bentonite. Applied Clay Science 23, 309–321.

Montes-H G., Fritz B., Clement A., 2004. Modeling of transport and reaction in an engineered barrier for radioactive waste confinement. Rapport ANDRA, CRP 0 CGS 04 001, p. 61.

Nagy, K.L., Cygan, R.T., Hanchar, J.M., Sturchio, N.C., 1999. Gibbsite growth kinetics on gibbsite, kaolinite, and muscovite: atomic force microscopy evidence for epitaxy and assessment of reactive surface area. Geochimica et Cosmochimica Acta 63 (16), 2337–2235.

Neaman, A., Pelletier, M., Villieras, F., 2003. The effects of exchanged cations, compression, heating and hydration on textural properties of bulk bentonite and its corresponding purified montmorillonite. Applied Clay Science 22, 153–168.

Nöack, Y., Collin, F., Nahon, D., Delvigne, J., Michaux, L., 1993. Secondary-mineral formation during natural weathering of pyroxene: review and thermodynamic approach. American Journal of Science 293, 111–134.

Poinssot, C., Toulhoat, P., 1998. Chemical interaction between a simulated nuclear waste glass and different backfill materials under a thermal gradient. Applied Geochemistry 13 (6), 715–773.

Rytwo, G., 1996. Exchange reactions in the Ca–Mg–Na-Montmorillonite system. Clays and Clay Minerals 44 (2), 276–285.

Sauzeat E., Guillaume D., Neaman A., Dubessy J., François M., Pfeiffert C., Pelletier M., Ruch R., Barres O., Yvon J., Villéras F. et Cathelineau M., 2001. Caractérisation minéralogique, cristallochimique et texturale de l'argile MX80. Rapport ANDRA No. CRP0ENG 01-001, p. 82.

Savage, D., Noy, D., Mihara, M., 2002. Modelling the interaction of bentonite with hyperalkaline fluids. Applied Geochemitry 17, 207–223.

Steefel, C.I., Lasaga, A.C., 1990. Permeability changes due to coupled flow and reaction. In: Melchior, D.C., Basset, R.L. (Eds.), Chemical Modelling of Aqueous Systems II American Chemical Society, Symposium Series, vol. 416, pp. 212–216.

Tournassat, C., Neaman, A., Villiéras, F., Bosbach, D., Charlet, L., 1995. Nanomorphology of montmorillonite particles: estimation of the clay edge sorption site density by low pressure gas adsorption and AFM observations. American Mineralogist 88, 1989–1989.

Ulm, F.J., Heukamp, F.H., Germaine, J.T., 2002. Residual design strength of cement-based materials for nuclear waste storage systems. Nuclear Engineering and Design 211, 51–60.

White, A.F., Peterson, M.L., 1990. Role of reactive-surface-area characterization in geochemical kinetic models. In: Melchior, D., Bassett, R. (Eds.), Chemicals modelling of aqueous systems II: Association of Chemical Society Symposium Series, vol. 416, pp. 461–475.